DMD Fast Forward. Published on December 12, 2008 as doi:10.1124/dmd.108.023432

DMD #23432

METABOLISM OF VORELOXIN (FORMERLY SNS-595), A NOVEL REPLICATION-DEPENDENT DNA DAMAGING AGENT

Marc J. Evanchik[1], Darin Allen[2], Josh C. Yoburn, Jeffrey A. Silverman and Ute Hoch[3]

Sunesis Pharmaceuticals, Inc., South San Francisco, CA 94080, USA

METABOLISM OF A NOVEL DNA DAMAGING AGENT

Marc J. Evanchik

Sunesis Pharmaceuticals, Inc.

341 Oyster Point Blvd.

South San Francisco, CA 94080

USA

(Phone) 408 421 9232

(Fax) 650 266 3501

evanchik.marc@gmail.com

Number of text pages: 37

Number of tables: 5

Number of figures: 5

Number of references: 26

Number of words in *Abstract*: 165

Number of words in *Introduction*: 322

Number of words in *Discussion*: 1000

Abbreviations used are:

Voreloxin, (+)-1,4-dihydro-7-(trans-3-methoxy-4-methylamino-1-pyrrolidinyl)-4-oxo-1-(2-thiazolyl)-1,8-naphthyridine-3-carboxylic acid; LC-MS/MS, liquid chromatography-tandem mass spectrometry; HPLC, high performance liquid chromatography; JVC,

jugular vein cannulated; BDC, bile duct cannulated; FVC, femoral vein cannulated; i.v., intravenous; UGT, UDP-glucuronosyltransferases, UDPGA, uridine 5'-diphosphoglucuronic acid; SPE, solid phase extraction; AUC, area under the curve. NADPH, nicotinamide adenine dinucleotide phosphate

Abstract

Voreloxin (formerly SNS-595 or AG-7352) is currently under investigation for the treatment of platinum-resistant ovarian cancer and acute myeloid leukemia (AML). In vitro voreloxin undergoes minimal cytochrome P450- and UGT-mediated metabolism, in vivo excretion of unchanged voreloxin as the major species is consistent with the slow rate of metabolism observed in vitro. The objective of the present study was to examine the cross-species metabolic profile of voreloxin and to identify and characterize the metabolites formed in rats. We also investigated baculovirus-expressed human P450s and UGTs to determine which isoforms participated in voreloxin metabolism. Incubations using human, monkey, and rat liver microsomes showed monkey and rat metabolism is similar to human. Voreloxin and metabolites collected from plasma, bile, and urine from rats administered radiolabeled voreloxin were separated by HPLC, and their structures elucidated by LC-MS/MS. Activity of metabolites was determined with authentic reference standards in cell-based cytotoxicity assays. The proposed structures of metabolites suggest that metabolic pathways for voreloxin include glucuronide conjugation, oxidation, N-dealkylation, and O-dealkylation.

Introduction

Voreloxin is a replication-dependent DNA damaging agent that intercalates DNA and inhibits topoisomerase II resulting in double-stranded DNA breaks, irreversible G2 arrest, and rapid apoptosis. The topoisomerase II-associated DNA intercalation and DNA damage produced by voreloxin is highly selective, and shows selectivity for proliferating cells. These targeted DNA-protein interactions may contribute to the broad clinical responses observed with voreloxin to date. The inhibition of topoisomerase II by voreloxin is differentiable from the actions of classic topoisomerase inhibitors including etoposide, doxorubicin and topotecan (Stockett et al., 2008). Voreloxin is a naphthyridine-derived small molecule that exists as a zwitterion containing carboxylic acid and amine functional groups, Figure1. Voreloxin is currently under clinical investigation in AML and ovarian cancer (Burris et al., 2007; Lancet et al., 2007).

Preclinical pharmacokinetic studies in rats and monkeys demonstrated that voreloxin has dose proportional exposure, low to moderate clearance, a moderate half-life and low inter-individual variability. In humans, pharmacokinetic estimates show dose linear increase in exposure, low clearance and a long half-life (Hoch and Silverman, 2007). In vitro studies using rat, monkey, and human liver microsomes indicated that voreloxin undergoes minimal oxidative and conjugative metabolism (Hoch et al., 2005). In addition, in vitro profiling suggests that rat metabolism is a good model of voreloxin human metabolism. In mass balance studies, greater than 90% of drug was eliminated within 48 hours of i.v. administration of 5 mg/kg [^{14}C]-voreloxin to rats, with a majority (~78 %) of the radioactivity recovered in the first 24 hours. Nearly 80 % of recovered

radioactivity was eliminated in the feces, and additional studies using bile duct-cannulated rats indicated biliary and direct intestinal secretion are routes of elimination (Hoch et al., 2005).

The current investigation focuses on the identification of in vivo metabolites collected after i.v. administration of voreloxin to male Sprague-Dawley rats. We observed 5 unique metabolites plus one degradation product of a phase I-mediated metabolite and two chemically rearranged isoforms of an acyl glucuronide.

Materials and Methods

Chemicals and Reagents. Except as specified below, all chemicals were purchased from Sigma-Aldrich (St. Louis, MO). HPLC solvents were analytical grade and purchased from EMD Chemicals (San Diego, CA). Flo-Scint III was used as the scintillation cocktail in on-line radioactivity detection and OptiPhase 'SuperMix' (PerkinElmer Life Sciences, Waltham, MA) was used for liquid scintillation counting. Voreloxin (, (+)-1,4-dihydro-7-[(3S,4S)-3-methoxy-4-(methylamino)-1-pyrroli- dinyl]-4-oxo-1-(2-thiazoyl)-1,8-naphthyridine-3-carboxylic acid) was synthesized at Dainippon Sumitomo Pharmaceutical Co., Ltd and was 99.9 % pure. [^{14}C]-voreloxin was synthesized with the radiolabel incorporated on the C-2 carbon of the naphthyridine ring with a specific activity of 137 μCi/mg and a radiochemical purity of 97.1%. Authentic metabolite standards of O-desmethyl-voreloxin, N-desmethyl-voreloxin, dihydrodecarboxylic acid-voreloxin were synthesized at Sunesis Pharmaceuticals, Inc., according to published procedures (Okada et al., 1993; Tomita et al., 2002), and had purities of greater than 90%. Pooled microsomes and expressed P450 and UGT enzymes were purchased from BD Biosciences (Woburn, MA)

Metabolite Profile In Vitro. To determine the cytochrome P450-dependent metabolite profile generated in the presence of liver microsomes, 1 or 10 μM voreloxin was incubated in the absence and presence of NADPH cofactor with pooled-sex liver microsomes from rats, monkeys, and humans. Incubations were performed in 100 mM sodium phosphate buffer, pH 7.4, containing 3.3 mM $MgCl_2$, 1 mg/mL liver microsomal protein, and 1 mM NADPH for 60 min. Metabolism of voreloxin by phase II UGT enzymes was investigated using liver microsome fractions supplemented with UDPGA

according to Fisher et.al. (2000). Reactions were for 60 minutes with 100 µM voreloxin, and initiated with 5 mM UDPGA. The pore forming agent alamethecin was added to liver microsomes at a concentration of 100 µg /mg protein and the mixture incubated for 30 min on ice prior to the addition of voreloxin and UDGPA. Saccharic acid (5 mM) was added to inhibit the action of glucuronidases on conjugates formed during the incubation. The oxidative metabolites were profiled using an API 4000 mass spectrometer coupled to a turbo electrospray ionization source. Prior to MS analysis chromatography was performed to achieve some degree of separation between the parent and the metabolites. Conjugative metabolites were profiled using a HPLC coupled to a UV detector set to 350 nm. The HPLC system consisted of an Agilent 1100 binary pump and a Phenomenex Synergi Hydro-RP column (150 x 2 mm, 4 micron, 80Å particle size). Mass spectral profiles of metabolites were obtained using two experiments: MS full scans to identify metabolites and selected ion scans to compare the metabolic profile across the three species.

To determine specific cytochrome P450 enzymes responsible for oxidative metabolism of voreloxin, baculovirus-expressed enzymes were employed. Individual P450 enzyme incubations were set up to contain one of the following enzymes: CYP3A4, 2D6, 2C9, 1A2, or 2C19. The amount of enzyme added to the incubation mixture was scaled so that the individual P450 activity was equal to the activity of that enzyme in the human liver microsome incubation. All other reaction conditions were identical to those described above. Baculovirus-expressed human UGT isoforms were screened to identify UGT enzymes capable of generating the glucuronide conjugates of voreloxin. The reaction

conditions were identical to those described above with UGTs substituted for liver microsomes. UGT isoforms screened included: 1A1, 1A4, 1A3, 2B7, 1A6, 1A9, 2B4, 1A8 and 1A10.

Rat Studies. In-life portions of the experiments were conducted according to institutional guidelines. Food and water were supplied ad libitum. Voreloxin was formulated in 4.5% sorbitol in water for injection with 0.17% methane sulfonic acid. To assess the route and rate of excretion, double bile-duct cannulated male Sprague Dawley rats weighing 225-275 g each received a single intravenous injection of 5 mg/kg voreloxin (3.7 MBq/kg) via the tail vein at 1 mL/kg. Bile was collected from 0 to 48 hours postdose in half hour intervals (0-2 hours), 1-hour intervals (2-4 hours), 2-hour intervals (4-8 hours), 16-hour interval (8-24 hours), and 24-hour interval (24-48 hours), while continuously replacing bile with blank bile taken from other rats at 1 mL/hr. During the same 48-hour period, urine and feces were collected in 24-hour intervals. For metabolite profiles, three bile duct- (BDC), jugular vein- (JVC), and femoral vein-cannulated (FVC) male Sprague Dawley rats weighing 225-275 g each received a single intravenous dose of 10 mg/kg [^{14}C]-voreloxin (specific activity of 50 µCi/kg). For elucidation of metabolites by LC-MS/MS, three FVC/BDC Sprague Dawley rats weighing 225-275 g each received a single intravenous dose of 10 mg/kg voreloxin. After administration of voreloxin, both groups of rats were handled identically, except that no plasma samples were collected from rats receiving unlabeled voreloxin. Rats were housed in metabolic cages to allow collection of bile, urine, and plasma. Blood samples were collected 5, 15, 30 min, 1, 2, 4, 8, and 12 hr post-dose via the JVC. After

blood sample removal an equal amount of donor blood was transfused via the JVC to replace the removed blood. Blood was collected on wet ice into K_2-EDTA tubes and plasma was harvested within 30 min after centrifugation of blood at 4 °C. Bile and urine were collected on dry ice in 2-hour intervals for the first 8 hours then between 8-12 hours post-dose. All samples were stored at -70 °C until analysis.

Pharmacokinetics. Total radioactivity in plasma from rats administered [^{14}C]-voreloxin was determined by addition of OptiPhase Supermix and subsequent measurement using a liquid scintillation counter (1450 Micobeta Trilux, Wallac). Voreloxin and metabolite concentrations in plasma samples were measured following protein precipitation with acetonitrile. Voreloxin was separated from metabolites on a reverse phase HPLC column with an Agilent 1100 system (Santa Clara, CA). Chromatography was carried out on a 250 x 4.6 mm 4 micron C18 Synergi Hydro column (Phenomenex, Torrance, CA) using a binary mobile phase consisting of a mixture of 0.1 % formic acid in water (solvent A) and acetonitrile (solvent B). The flow rate was 0.75 mL/min with the following gradient: solvent A/solvent B 90:10 for 2 min; changed from 90:10 to 70:30 from 2 to 45 min; changed from 70:30 to 10:90 from 45 to 47 min; held at 10:90 from 47 to 49 min, changed from 10:90 to 90:10 from 49 to 50 min, held at 90:10 from 50 to 52 min, changed from 90:10 to 10:90 from 52 to 55 min, changed from 10:90 to 90:10 from 55 to 57 min; the column was allowed to equilibrate at 90:10 before the next injection. The HPLC was coupled to a Radiomatic 610TR Flow Scintillation Analyzer equipped with a 500 µL liquid cell (PerkinElmer Life Sciences, Waltham, MA). A quantitative assessment of individual radiolabeled peaks in the plasma was made by multiplying the

percent peak area of the compound of interest by the total quantified radioactivity. Pharmacokinetic parameters were analyzed with WinNonlin v4.1 (Pharsight, Mountain View, CA) software using noncompartmental analysis. The following parameters were estimated: $T_{½}$, C_0, AUC_{last}, $AUC_{0\text{-}inf}$, CL, and $V_{ss.}$

Routes and Rate of Excretion. Radioactivity in urine and bile was counted directly after addition of tissue-dissolving solution and scintillation liquid. Radioactivity in feces was determined after combustion. Radioactivity in each sample was measured for 5 minutes with a liquid scintillation counter.

Metabolite Identification. Metabolites were characterized in plasma, urine, and bile samples collected from rats receiving voreloxin. Urine samples were analyzed without further preparation. Bile samples were diluted in water prior to injection at a 1:50 ratio. Plasma samples were extracted using the same acetonitrile protein precipitation method used in the pharmacokinetic analysis described. Lower limits of detection for voreloxin and metabolites M1, M2a, M3,and M4 were determined using standard curves prepared by spiking compound in plasma. For the proposed acyl glucronide metabolite, M1, the concentration of the plasma spiked standards was also compared against non extracted samples of the same concentration. Aliquots of urine and bile samples from each time interval collected were analyzed by reverse-phase HPLC-MS/MS using the HPLC gradient system and column described above.

The characterization of metabolites was performed with an API4000 (Sciex/ABI, Foster City, CA) triple quadrupole mass spectrometer using turbo electrospray ionization operated in positive ion mode with the following source parameters: source temperature 650 °C, ion spray voltage 5.5 kV, and declustering potential set to 46 V.

Isolation of Voreloxin Glucuronide. Voreloxin glucuronide adduct was isolated from rat bile collected between 0-12 hours post administration using solid phase extraction (SPE). A strata-x 6 mL column (Phenomenex, Torrance, CA) was preconditioned with 6 mL methanol followed by 6 mL of water. One mL of bile was loaded and rinsed with 6-10 mL of water. Analytes were eluted from the column with methanol and collected in silanized glass tubes, evaporated to dryness under nitrogen, and reconstituted in 50/50 acetonitrile/0.17% methane sulfonic acid in water solution. The samples were reconstituted then separated using reverse chromatography as described above. Samples were freeze dried overnight using a lyophilizer (VirTis, Gardiner, NY) kept frozen at -20°C until reconstituted and analyzed.

Cleavage of Voreloxin Glucuronide. Glucuronide conjugate isolated from rat bile was subjected to cleavage under acidic and basic conditions, and with β-glucuronidase. Freeze-dried conjugate was reconstituted in water to a concentration of 0.1 mg/mL. For cleavage under acidic and basic conditions, an aliquot of the isolated glucuronide (100 µL) was incubated with HCl or NaOH at a final concentration of 0.1 N for 30 min at 37 °C. For β-glucuronidase cleavage, a 100 µL aliquot of the reconstituted glucuronide was added to 100 µL of 100 mM sodium phosphate buffer, pH 7.4 to achieve a final activity of 5000 units/mL β-glucuronidase from *Escherichia coli* (Sigma, St. Louis, MO) and

incubated at 37 °C for 30 min. Control samples were treated similarly but without the addition of acid, base, or β-glucuronidase. Acidic and basic reactions were stopped by addition equal molar base or acid, to return the reaction mixture to neutral pH, and immediately analyzed. Reactions with β-glucuronidase were terminated by the addition of an equal volume of ACN followed by analysis. Samples were chromatographically separated on a reverse phase HPLC column with an Agilent 1100 system (Santa Clara, CA) coupled to a UV detector set to 350 nm. Separation of the glucuronide conjugate and voreloxin was achieved on a 150 x 4.6 mm 4 micron C18 Synergi Hydro column (Phenomenex, Torrance, CA) using mobile phase A of 0.1 % formic acid in water and mobile phase B, acetonitrile. The flow rate was 0.8 mL/min with the following gradient: 0-1 min hold at 5 % B followed by a linear gradient to 50 % B at 7 min and held for 1 min; 8-9 min ramping to 5% B and held for the completion of the run.

Synthesis of Metabolite M2a. Metabolite M2a was synthesized in a manner analogous to that of a similar compound (Tsuzuki et al., 2004a). Voreloxin was *N*-protected with di-*tert*-butyl dicarbonate in 1 M NaOH, treated with $NaBH_4$ in MeOH, followed by 1 M HCl to give 7-[(*S*,S)-3-amino-4-methoxy-pyrrolidin-1-yl]-1-thiazol-2-yl-2,3-dihydro-1H-[1,8]naphthyridin-4-one hydrochloride (metabolite M2a.)

Synthesis of Metabolite M3 and M4. The *N*- and *O*-des-methyl metabolites were synthesized in a manner corresponding to an earlier reported synthesis of voreloxin (Tsuzuki et al., 2004b). (*S,S*)-3-tert-Butoxycarbonylamino-4-hydroxy-pyrrolidine-1-carboxylic acid tert-butyl ester was selectively *O*-methylated with NaH and MeI in THF

then deprotected with HCl in dioxane to give the (*S*,*S*)-3-amino-4-methoxy-pyrrolidine dihydrochloride needed for synthesis of metabolite M3. The same (*S*,*S*)-3-tert-butoxycarbonylamino-4-hydroxy-pyrrolidine-1-carboxylic acid tert-butyl ester was *O*-protected as a silyl ether with TBDMSCl and imidazole in DCM, *N*-methylated with NaH and MeI in DMF, and deprotected by TBAF in THF followed by HCl in dioxane to give the (*S*,*S*)-3-methylamino-4-hydroxy-pyrrolidine dihydrochloride needed for synthesis of metabolite M4. The above intermediates were taken on to 1,4-dihydro-7[(*S*,*S*)-3-amino-4-methoxy-pyrrolidinyl]-4-oxo-1-(2-thiazolyl)-1,8-naphthyridine-3-carboxylic acid (metabolite M3) and 1,4-dihydro-7[(*S*,*S*)-3-hydroxy-4-methylamino-pyrrolidinyl]-4-oxo-1-(2-thiazolyl)-1,8-naphthyridine-3-carboxylic acid (metabolite M4) as previously described (Tsuzuki et al., 2004a).

Activity of Voreloxin and Metabolites. Cell proliferation assays were performed using the MTT ((3-(4,5)-Dimethylthiazol-2-yl)-2,5-diphenyltetrazolium bromide) cytotoxicity assay as previously described (Mosmann, 1983; Hansen et al., 1989). Briefly, 96-well tissue culture-treated flat bottom plates (Costar #3595) were plated with 4000 trypsinized HCT 116 cells at 100 µL/well and incubated overnight. Stock concentrations (100x) of voreloxin and metabolite reference standards were prepared in DMSO at 5 µM and serially diluted two-fold in DMSO in a 96-well polypropylene v-bottom plate (Costar #3363). DMSO dilutions (5 µL) were then added to 45 µL supplemented RPMI 1640, and 10 µL/well of this mixture were added to plates containing HCT 116 cells. Plates were incubated for 72 hours at 37 ^{o}C in an incubator (5% CO_2). Cell viability was then recorded as the difference in absorbance at 595 nm between compound- and DMSO-

treated cells using a Biorad Benchmark Microplate Reader (Hercules, CA). Data were plotted and IC_{50} values calculated using least squares regression using Prism 4 software (Graphpad, La Jolla, CA).

Results

Metabolite profiles after microsomal incubations. Incubation of voreloxin with liver microsomes from human, monkey, and rat in the presence of NADPH resulted in the formation of three metabolites M2a, M3, and M4, suggesting involvement of cytochrome P450 enzymes in voreloxin metabolism. Previous studies monitoring voreloxin stability after 60 minutes incubation showed >97%, >74%, and >85% unchanged voreloxin remained after incubation with human, monkey, and rat liver microsomes, respectively (data not shown). Formation of these metabolites was similar across the species tested, with metabolite M4 being the most prevalent species. Metabolites M2a, M3, and M4 had MH^+ molecular ions at m/z 360, 388, and 388, respectively. To assess which human P450 enzymes mediate the metabolism seen in human liver microsomes, voreloxin was incubated with Supersomes™ containing individually expressed cytochrome CYP3A4, 2D6, 2C9, 2C19 or 1A2 enzymes. The results show that CYP3A4, 2D6, and 1A2 play a role in the cytochrome P450-mediated metabolism of voreloxin. Cytochrome P450s 2C9 and 2C19 do not contribute to the in vitro metabolism of voreloxin.

When incubated with liver microsomes in the presence of UDPGA, voreloxin formed one metabolite, M1. The M1 metabolite was formed in the presence of both human, and rat, liver microsomes. Incubation of voreloxin with baculovirus-expressed human UGT isoforms indicated several UGT isoforms, including UGT1A1, 1A4, 1A3, 2B7, 2B15, and 1A8, were capable of conjugating voreloxin. UGT isoforms that showed little or no metabolic activity against voreloxin included 2B17, 2B4, 1A6, 1A10, and 1A9.

Pharmacokinetics of Total Radioactivity and Voreloxin. The plasma concentration-time profiles of total radioactivity and voreloxin after intravenous administration to rats is shown in Figure 2. Pharmacokinetic parameters are summarized in Table 1. Plasma concentration-time profiles for voreloxin and total radioactivity were similar, declined in a biphasic fashion, and resulted in terminal half-lives of 6.3 hr and 5.4 hr, respectively. Pharmacokinetic parameters were similar for voreloxin and total radioactivity, with a maximum plasma concentration at time zero (C0) of 4.2 µgEq /mL, area under the concentration-time-curve (AUC) of 17 µgEq*hr/mL, clearance of 10 mL/min/kg, and a volume of distribution at steady state of 4 L/kg.

Routes and Rate of Excretion. Bile, urine, and fecal excretion after intravenous administration of [^{14}C]-voreloxin in rats are summarized in Table 2. Forty-eight hours after IV injection 37.9%, 32.5%, and 19.6% of the administered radioactivity were excreted into the bile, feces, and urine, respectively. Biliary excretion followed a logarithmic pattern, with half the radioactivity excreted by 6 hours post dose. In bile and urine, the majority of radioactivity was recovered by 24 hours post dose, while radioactivity in feces continued to increase between 24 and 48 hours post dose. Together with the small amounts of radioactivity recovered in the carcass, total recoveries of radioactivity were >95% of the dose within the first 48 hours.

Metabolite Profiles in Plasma, Urine, and Bile. HPLC radiochromatograms from plasma (4 hr), urine (6-8 hr), and bile (4-6 hr) after a 10 mg/kg bolus i.v. injection of [^{14}C]-voreloxin are shown in Figure 3. Based on the retention time, voreloxin (P) was the

largest peak observed in plasma, urine, and bile. One additional metabolite peak (M4) was observed in plasma. In urine, six metabolite peaks were detected in addition to voreloxin (M1, M2, M3, M2a, M4, and M5). In addition to five of the metabolite peaks detected in urine, two additional peaks (M1a and M1b) were observed in bile. Metabolite peak M2 was not observed in the depicted bile sample, but was observed at other collection intervals. The contribution of voreloxin and its metabolites to total radioactivity over the 12 hour collection interval is summarized in Table 3. Parent drug was the predominant component, accounting for 97 %, 35 %, and 30 % of the radioactivity in plasma, urine, and bile, respectively. The remaining radioactivity in plasma (3 %) was due to M2. In urine, metabolite peaks M4, M5, M2a and M1 accounted for 16, 15, 12, and 10% of the radioactivity, respectively. Metabolite peaks M2 and M3 were minor, and each accounted for 3 % of the total radioactivity. In bile, metabolite peaks M5, M1, M2a, and M1b accounted for 17, 14, 12, and 10 % of the total radioactivity, respectively. Total radioactivity of metabolite peaks M1a, M4, M2, and M3 accounted for less than 10% each.

Identification of Voreloxin Metabolites. Voreloxin metabolites in rat bile were structurally characterized using triple quadrupole LC/MS/MS. Protonated molecules, MS/MS spectra, and proposed structures are summarized in Table 4. The LC-MS/MS spectrum for voreloxin is shown in Figure 4. In addition to the MH^+ molecular ion at m/z 402, predominant product ions with m/z 384, 332, 269, and 243 were observed. The molecular ion at m/z 384 was the result of a loss of water (18 amu) from voreloxin. Loss of 70 amu (carboxylic acid and C-2/C-3 atoms of the naphthyridinone ring) generated the

product ion with m/z 332. Additional loss of the N- and O-methyl substituents on the pyrrolidine ring coupled with saturation on the pyrolidine ring resulted in the product ion with m/z 269. The product ion at m/z 243 is consistent with a core fragment of the naphthyridine ring. The minor product ion at m/z 274 resulted from cleavage at the pyrolidine-nitrogen.

Metabolite peak M1 had a MH^+ molecular ion at m/z 578 and generated a fragment ion at m/z 402, resulting from the loss of 176 amu, diagnostic of a glucuronide conjugate. Additional product ions observed at m/z 384, 332, and 269 were identical to the product ions of voreloxin, supporting the identification of M1 as glucuronide adduct. Metabolite M1 isolated from bile collected from rats dosed with voreloxin underwent hydrolysis upon treatment with β-glucuronidase. Disappearance of the metabolite peak corresponded to a 1:1 appearance of a voreloxin peak. Moreover, treatment of M1 with 0.1 N sodium hydroxide or 0.1 N hydrochloric acid resulted in complete disappearance of the metabolite peak within 30 minutes. These results supported the notion that M1 was an ester glucuronide. Metabolites M1a and M1b showed identical molecular and product ions to M1, also suggesting they were glucuronide metabolites.

Metabolite M2 showed a MH^+ molecular ion at m/z 404, an addition of 2 amu compared to voreloxin. Predominant product ions observed were at m/z 360, 306, and 243. The molecular ion at m/z 360 was consistent with loss of the carboxylic acid moiety (44 amu). Additional loss of the N- and O-methyl substituents on the pyrrolidine ring led to the product ion at m/z 297. The product ions at m/z 217 and 247 were consistent with

cleavage at the pyrrolidine-nitrogen. The structure of this metabolite could not be confirmed since a synthetic reference standard was not available.

A product ion spectrum related to that of metabolite M2 was observed for metabolite M2a. The molecular ion for this metabolite was at m/z 360, indicating a loss of the carboxylic acid compared to metabolite M2. Similar to metabolite M2, metabolite M2a generated product ions at m/z 318, 306, 297, 243, 217, 205, and 193. Identity of metabolite M2a as dihydro-decarboxylic acid voreloxin was confirmed with an authentic reference standard, which shared identical retention time and MS/MS spectrum with M2a.

Metabolite M4 had a MH^+ molecular ion at m/z 388, indicating a loss of 14 amu compared to voreloxin. The fragmentation pattern for M4 was similar to that of voreloxin and included loss of water (18 amu) to result in a product ion at m/z 370, loss of 70 amu to result in a product ion at m/z 318, and formation of the product ions at m/z 269 and 243 also observed for voreloxin. Chemically synthesized N-desmethyl-voreloxin had the same retention time as M4 and showed an identical fragmentation pattern upon MS/MS analysis, confirming identity of M4 as N-desmethyl-voreloxin.

Metabolite M3 also had a MH^+ molecular ion at m/z 388, indicating a loss of 14 amu compared to voreloxin. The fragmentation pattern for M3 was identical to that observed for M4. Chemically synthesized O-desmethyl-voreloxin had the same retention time as M3 confirming the identity of M3 as O-desmethyl-voreloxin. Metabolite M5 did not

yield a detectable molecular ion when subjected to mass spectral analysis; no structure could therefore be proposed for this non-polar metabolite.

LC-MS/MS analysis of plasma and urine samples confirmed the identity of the metabolite peaks shown in Figure 3 as those described for bile. Lower limit of detection for metabolites for which standards were available, were at least 5 ng/mL. Peak area response for the glucuronide metabolite, M1, spiked in plasma prior to extraction was identical to glucuronide prepared in pure solution at the same concentrations.

Cytotoxicity of Voreloxin and Metabolites. Cytotoxicity of voreloxin, dihydrodecarboxylic acid voreloxin (M2a), O-desmethyl-voreloxin (M3), and N-desmethyl-voreloxin (M4) is summarized in Table 5. N-Desmethyl-voreloxin showed activity that was similar to that of voreloxin, whereas the O-desmethyl and the dihydrodecarboxylic acid metabolites were inactive at the highest concentrations tested.

Discussion

Voreloxin (formerly SNS-595) is a novel naphthyridine analog, currently under investigation for the treatment of platinum-resistant ovarian cancer and acute myloid leukemia. The present study describes the pharmacokinetics and metabolism of this novel chemotherapeutic. Pharmacokinetic parameters of voreloxin in nonclinical studies showed a favorable profile; systemic clearance was low at 11% of the rat liver blood flow, volume of distribution at steady state was high, indicating distribution outside the vasculature, and terminal half-life was 5.4 hours. Pharmacokinetic estimates based on voreloxin were similar to those determined based on total radioactivity, suggesting low levels of circulating metabolites. Indeed, a more detailed analysis of plasma samples confirmed that voreloxin contributed to 97 % of the radioactivity in plasma.

In vitro metabolism of Voreloxin was studied in microsomes from rat and monkey, the two species used in nonclinical toxicology studies, and compared to that in microsomes from human. Voreloxin is relatively stable to oxidative and conjugative metabolism. In microsomes supplemented with NADPH, greater than 85, 74, and 97% of parent drug remain after an hour with either 1 or 10 μM voreloxin, in rat, monkey, and human microsomes, respectively. We observed O- and N-desmethyl-voreloxin and dihydrodecarboxylic acid voreloxin in rat, monkey, and human microsomal incubations. In all species the N-desmethyl metabolite, M4, was the predominant species observed based on area under the curve of the ionized species. Both rat and human microsomes were capable of generating a glucuronide conjugate of voreloxin in microsomes

supplemented with UDGPA, but high concentrations (100 μM) of voreloxin were required to observe this metabolite, suggesting that its binding affinity to the UGT enzyme(s) is weak. Metabolite M5 was not observed in microsomal incubations supplemented with either NADPH or UDGPA. Cross-species comparison of the oxidative and conjugative metabolite profiles after microsomal incubation indicates that microsomal metabolism in the rat is a good predictor of human microsomal metabolism.

We used baculovirus-expressed human P450 enzyme preparations, to predict which enzyme(s) are responsible for generating the observed oxidative metabolites. Incubations containing human CYP3A4, 2D6, 2C9, 1A2, or 2C19 showed that 3A4 and 1A2 are capable of generating the N desmethyl, O-desmethyl and dihydrodecarboxylic acid metabolites. Cytochrome CYP2D6 generated the dihydrodecarboxylic acid metabolite, M2a, likely through oxidation of voreloxin to the dihydro species, M2, which chemically degrades to M2a. Cytochrome CYP1A2 was also important in that along with CYP3A4 was the only other isoform capable of generating all of the oxidative metabolites.

Identification of the metabolites in rat bile allowed us to propose the metabolic scheme shown in Figure 5. Metabolites identified by LC-MS/MS analysis and synthesized reference standards include N-desmethyl-voreloxin, O-desmethyl-voreloxin, and dihydrodecarboxylic acid voreloxin. While N- and O-desmethyl-voreloxin are primary metabolites, the diyhdrodecarboxylic acid metabolite, M2a, is likely a degradation product of dihydro-voreloxin (metabolite M2). Low-level presence of a species at m/z

404, a molecular weight consistent with the proposed structure for M2, and the commonly observed instability of β-ketoacids, support this hypothesis.

For many xenobiotics, glucuronidation constitutes a major route of elimination and is the second most common clearance mechanism listed for the top 200 most prescribed drugs on the market (Williams et al., 2004). Most common conjugations occur at hydroxyl, amino, and carboxylic acid centers but conjugation at carbon centers has been observed (Miners et al., 2004). In the case of carboxylate conjugation, the biologically generated 1-*O*-β glucuronide metabolite, unlike other types of glucuronides, is relatively labile in vitro and in vivo and can also undergo chemical rearrangement of the glucuronide to form isomers of the acyl glucuronide (Spahn-Langguth and Benet, 1992; Wang and Dickinson, 1998). In the acyl migration, the aglycone is transferred to the C-2, C-3, or C-4 position of the glucuronic acid ring (Spahn-Langguth et al., 1996; Bailey and Dickinson, 2003).

Here, identity of metabolite M1 as the acyl glucuronide of voreloxin could not be definitively confirmed via a synthesized reference standard. Chemical synthesis was attempted, but failed to yield the desired glucuronide. The limited solubility of voreloxin in appropriate solvents prevented direct glucuronidation reactions. Addition of protecting groups on the secondary amine functionality increased the solubility of voreloxin sufficiently to allow the formation of the acyl glucuronide. However, attempts to remove the protecting group also resulted in cleavage of the desired glucuronide. Nevertheless, several lines of evidence support identification of metabolite M1 as the acyl glucuronide

of voreloxin: (1) Acyl glucuronidation is commonly described for carboxylic acid-containing drugs, including fluoroquinolone antibiotics (Dalvie et al., 1996; Ramji et al., 2001; Tachibana et al., 2005), which are structurally related to voreloxin; (2) A glucuronide isolated from rat bile was relatively labile and completely converted to voreloxin under acidic and basic conditions, and after incubation with β-glucuronidase; (3) The presence of multiple peaks for M1 in bile and not in urine suggests possible intra-acyl rearrangement of the acyl glucuronide in a pH-dependent manner. Intramolecular rearrangement of acyl glucuronides occurs more readily under the alkaline conditions of bile (Hyneck et al., 1988; Frank et al., 1989).

Radioactivity was observed in bile, urine and feces, indicating that voreloxin is removed through hepatic clearance (38%), renal clearance (20%), and by direct intestinal secretion (33%). In urine and bile, unchanged voreloxin contributed to 35% and 30% of the radioactivity and constituted the largest single peak. Formation of metabolites M2/M2a, M3, and M4 is most likely mediated by the cytochrome P450 system. This pathway of elimination contributed 34% and 21% of the radioactivity in urine and bile, respectively. Finally, elimination by UGT glucuronosyltransferases contributed to 10% and 32% of the radioactivity in urine and bile, respectively. Among the metabolites, only N-desmethyl-voreloxin was detected in plasma. This metabolite showed potency equal to that of voreloxin in a cytotoxicity assay, but is present at only relatively low levels.

In conclusion, in the present study voreloxin showed favorable pharmacokinetic properties in nonclinical species. Elimination occurred renally, hepatically, as well as by

direct intestinal secretion. Four primary metabolites were identified and the human enzymes capable of producing them profiled. In rats, excretion of unchanged voreloxin, phase II and P450-mediated metabolism played roles in the excretion of voreloxin.

References

Bailey MJ and Dickinson RG (2003) Acyl glucuronide reactivity in perspective: biological consequences. *Chem Biol Interact* **145:**117-137.

Benet LZ, Spahn-Langguth H, Iwakawa S, Volland C, Mizuma T, Mayer S, Mutschler E and Lin ET (1993) Predictability of the covalent binding of acidic drugs in man. *Life Sci* **53:**PL141-146.

Bolze S, Bromet N, Gay-Feutry C, Massiere F, Boulieu R and Hulot T (2002) Development of an in vitro screening model for the biosynthesis of acyl glucuronide metabolites and the assessment of their reactivity toward human serum albumin. *Drug Metab Dispos* **30:**404-413.

Burris H, Krug L, Shapiro G, Fidias P, Crawford J, Reiman T, Michelson G, Berman C, Mahadocon K, Hoch U, Adelman D and Ettinger D (2007) SNS-595: Preliminary Results Of Two Phase 2 Second Line Studies In Lung Cancer [abstract], in: *ECCO 14 - European Cancer Conference*, Bacelona, Spain.

Dalvie DK, Khosla NB, Navetta KA and Brighty KE (1996) Metabolism and excretion of trovafloxacin, a new quinolone antibiotic, in Sprague-Dawley rats and beagle dogs. Effect of bile duct cannulation on excretion pathways. *Drug Metab Dispos* **24:**1231-1240.

Fisher MB, Campanale K, Ackermann BL, VandenBranden M and Wrighton SA (2000) In vitro glucuronidation using human liver microsomes and the pore-forming peptide alamethicin. *Drug Metab Dispos* **28:**560-566.

Frank SK, Mathiesen DA, Szurszewski M, Kuffel MJ and Ames MM (1989) Preclinical pharmacology of the anthrapyrazole analog oxantrazole (NSC-349174, piroxantrone). *Cancer Chemother Pharmacol* **23:**213-218.

Hansen MB, Nielsen SE and Berg K (1989) Re-examination and further development of a precise and rapid dye method for measuring cell growth/cell kill. *J Immunol Methods* **119:**203-210.

Hoch U, Evanchik MJ and Silverman JA (2005) CYP450 Inhibition, Induction, Metabolism and Routes of Elimination of SNS-595, a Novel Cell Cycle Inhibitor Currently in Phase I Clinical Trials [abstract], in: *AACR-NCI-EORTC International Conference: Molecular Targets and Cancer Therapeutics*, pp C221, Philadelphia, Pennsylvania.

Hoch U and Silverman JA (2007) SNS-595 demonstrates predictable, dose-proportional pharmacokinetics in three Phase 1 clinical studies [abstract], in: *AAPS Annual Meeting and Exposition*, pp 3658, American Association of Pharmaceutical Scientists, San Diego, CA.

Hyneck ML, Munafo A and Benet LZ (1988) Effect of pH on acyl migration and hydrolysis of tolmetin glucuronide. *Drug Metab Dispos* **16:**322-324.

Lancet J, Kantarjian H, Ravandi F, Bastien S, Alino K, Michelson G and Karp J (2007) SNS-595 Demonstrates Clinical Responses in a Phase 1 Study in Acute Leukemia [abstract], in: *Blood (ASH Annual Meeting Abstracts)*, pp 442, American Society of Hematology, Atlanta, Georgia.

Miners JO, Smith PA, Sorich MJ, McKinnon RA and Mackenzie PI (2004) Predicting human drug glucuronidation parameters: application of in vitro and in silico modeling approaches. *Annu Rev Pharmacol Toxicol* **44:**1-25.

Mosmann T (1983) Rapid colorimetric assay for cellular growth and survival: Application to proliferation and cytotoxicity assays. *Journal of Immunological Methods* **65:**55-63.

Okada T, Sato H, Tsuji T, Tsushima T, Nakai H, Yoshida T and Matsuura S (1993) Synthesis and structure-activity relationships of 7-(3'-amino-4'-methoxypyrrolidin-1'-yl)-1-cyclopropyl-6,8-difluoro-1,4- dihydro-4-oxoquinoline-3-carboxylic acids. *Chem Pharm Bull (Tokyo)* **41:**132-138.

Ramji JV, Austin NE, Boyle GW, Chalker MH, Duncan G, Fairless AJ, Hollis FJ, McDonnell DF, Musick TJ and Shardlow PC (2001) The disposition of gemifloxacin, a new fluoroquinolone antibiotic, in rats and dogs. *Drug Metab Dispos* **29:**435-442.

Spahn-Langguth H and Benet LZ (1992) Acyl glucuronides revisited: is the glucuronidation process a toxification as well as a detoxification mechanism? *Drug Metab Rev* **24:**5-47.

Spahn-Langguth H, Dahms M and Hermening A (1996) Acyl glucuronides: covalent binding and its potential relevance. *Adv Exp Med Biol* **387:**313-328.

Stockett D, Byl JA, Hawtin RE, Tan N, Zhu Y, Arkin MR, Yang W, McDowell RS, Osheroff N and Fox JA (2008) SNS-595 is a potent anti-tumor agent that has a dual mechanism of action: DNA intercalation and site-selective topoisomerase II poisoning [abstract], in: *Proceedings of the 99th Annual Meeting of the American*

Association for Cancer Research, pp 1860, American Association for Cancer Research, San Diego, CA.

Tachibana M, Tanaka M, Masubuchi Y and Horie T (2005) Acyl glucuronidation of fluoroquinolone antibiotics by the UDP-glucuronosyltransferase 1A subfamily in human liver microsomes. *Drug Metab Dispos* **33:**803-811.

Terrier N, Benoit E, Senay C, Lapicque F, Radominska-Pandya A, Magdalou J and Fournel-Gigleux S (1999) Human and rat liver UDP-glucuronosyltransferases are targets of ketoprofen acylglucuronide. *Mol Pharmacol* **56:**226-234.

Tomita K, Tsuzuki Y, Shibamori K, Tashima M, Kajikawa F, Sato Y, Kashimoto S, Chiba K and Hino K (2002) Synthesis and structure-activity relationships of novel 7-substituted 1,4-dihydro-4-oxo-1-(2-thiazolyl)-1,8-naphthyridine-3-carboxylic acids as antitumor agents. Part 1. *J Med Chem* **45:**5564-5575.

Tsuzuki Y, Tomita K, Sato Y, Kashimoto S and Chiba K (2004a) Synthesis and structure-activity relationships of 3-substituted 1,4-dihydro-4-oxo-1-(2-thiazolyl)-1,8-naphthyridines as novel antitumor agents. *Bioorg Med Chem Lett* **14:**3189-3193.

Tsuzuki Y, Tomita K, Shibamori K, Sato Y, Kashimoto S and Chiba K (2004b) Synthesis and structure-activity relationships of novel 7-substituted 1,4-dihydro-4-oxo-1-(2-thiazolyl)-1,8-naphthyridine-3-carboxylic acids as antitumor agents. Part 2. *J Med Chem* **47:**2097-2109.

Wang M and Dickinson RG (1998) Disposition and covalent binding of diflunisal and diflunisal acyl glucuronide in the isolated perfused rat liver. *Drug Metab Dispos* **26:**98-104.

Williams JA, Hyland R, Jones BC, Smith DA, Hurst S, Goosen TC, Peterkin V, Koup JR and Ball SE (2004) Drug-drug interactions for UDP-glucuronosyltransferase substrates: a pharmacokinetic explanation for typically observed low exposure (AUCi/AUC) ratios. *Drug Metab Dispos* **32:**1201-1208.

Footnotes

[1] Current affiliation: ChemoCentryx, Inc., Mountain View, CA USA

[2] Current affiliation: Gilead Sciences, Inc., Foster City, CA USA

[3] Current affiliation: Nektar Therapeutics, Inc., San Carlos, CA USA

Figure Legends

Figure 1. Structure of [^{14}C]-voreloxin

Figure 2. Pharmacokinetics of total radioactivity and voreloxin

Figure 3. Representative radiochromatograms of voreloxin (P) and its metabolites (M#) in plasma (A), urine (B), and bile (C) after a 10 mg/kg bolus intravenous injection of [^{14}C]-voreloxin to rats.

Figure 4. Representative LC-MS/MS spectra of voreloxin in rat bile.

Figure 5. Proposed metabolic pathways for voreloxin in rat.

Table 1. Mean (S.D.) pharmacokinetic parameters for total radioactivity and voreloxin in rats after IV administration of 10 mg/kg [^{14}C]-voreloxin (n=3)

	$T_{1/2}$ (hr)	C_0 (µgEq/mL)	AUC_{inf} (µgEq*hr/mL)	CL (mL/min/kg)	V_{ss} (L/kg)
Voreloxin	5.4±1.0	4.3±0.9	17±2	10±1	4±0.3
Total Radioactivity	6.3±0.7	4.2±1.4	17±3	10±2	5±0.4

DMD Fast Forward. Published on December 12, 2008 as DOI: 10.1124/dmd.108.023432
This article has not been copyedited and formatted. The final version may differ from this version.

Table 2. Urinary, Fecal, and Bile Excretion of Radioactivity After a Single IV Dose of [^{14}C]-Voreloxin to Bile-Duct Cannulated Rats at 5 mg/kg

Sample[a]	**Cumulative Excretion ± SEM (% Dose) at Specific Time Points**									
	0-0.5 hr	**0-1 hr**	**0-1.5 hr**	**0-2 hr**	**0-3 hr**	**0-4 hr**	**0-6 hr**	**0-8 hr**	**0-24 hr**	**0-48 hr**
Bile	2.8±0.4	5.6±1.2	8.0±2.0	10.3±2.3	14.1±2.2	17.2±2.3	21.8±2.4	25.0±2.4	35.2±2.6	37.9±2.7
Urine	nd	nd	nd	nd	nd	nd	nd	nd	17.4±0.2	19.6±0.7
Feces	nd	nd	nd	nd	nd	nd	nd	nd	20.8±1.7	32.5±4.4
Carcass	nd	nd	nd	nd	nd	nd	nd	nd	nd	6.0±1.4
Total	**2.8±0.4**	**5.6±1.2**	**8.0±2.0**	**10.3±2.3**	**14.1±2.2**	**17.2±2.3**	**21.8±2.4**	**25.0±2.4**	**73.4±2.1**	**95.9±0.4**

nd = not determined.

[a]n = 3/group.

Table 3. Mean percent peak area of [^{14}C]-voreloxin-related radiolabeled peaks found in rat urine and bile.

Peak	Retention Time	**Mean % of dose**	
		Urine	**Bile**
M1a	17.6	**N.D.**[a]	**8**
M1b	19.2	**N.D.**	**10**
M1	20.5	**10**	**14**
M2	26.6	**3**	**2**
M3	29.5	**3**	**1**
M2a	34.4	**12**	**12**
M4	38.7	**16**	**6**
Voreloxin	39.5	**35**	**30**
M5	49.9	**15**	**17**

[a] N.D., not detected

Table 4. Summary of structural information obtained by LC-MS/MS for metabolites of voreloxin in rat plasma, bile, and urine

Peak	Retention Time	$[M+H]^+$	MS/MS Fragment Ions	Additional Analysis	Metabolite Identity
M1a	17.6	578	402, **384**, 332, 267	-[a]	Acyl glucuronide of voreloxin
M1b	19.2	578	402, **384**, 332, 267	-	Acyl glucuronide of voreloxin
M1	20.5	578	402, **384**, 332, 267	Cleavage w/ β-glucuronidase, OH^-	Acyl glucuronide of voreloxin
M2	26.6	404	360, 318, **307**, 297, 247, **243**, 217, 205	-	Dihydro-voreloxin
M3	29.5	388	370, **318**, 269, 243	Chemical standard	O-Desmethyl-voreloxin
M2a	34.4	360	318, 307, 302, **297**, 369, 260, 247, **243**, 217, 205, 193	Chemical standard	Dihydrodecarboxylic acid voreloxin
M4	38.7	388	370, **318**, 269, 243	Chemical standard	N-Desmethyl-voreloxin
Voreloxin	39.5	402	384, **332**, 269, 243, 231	Parent drug	Voreloxin
M5	49.9	N.D.[b]	-	-	Unknown

[a] -, not performed; [b] N.D., not determined

DMD Fast Forward. Published on December 12, 2008 as DOI: 10.1124/dmd.108.023432
This article has not been copyedited and formatted. The final version may differ from this version.

Table 5. Cytotoxicity of voreloxin and metabolites M2a, M3, and M4.

	IC50 (μM)			
	Voreloxin	M2a	M3	M4
HCT 116	0.42	>5	>5	0.51

Figure 1

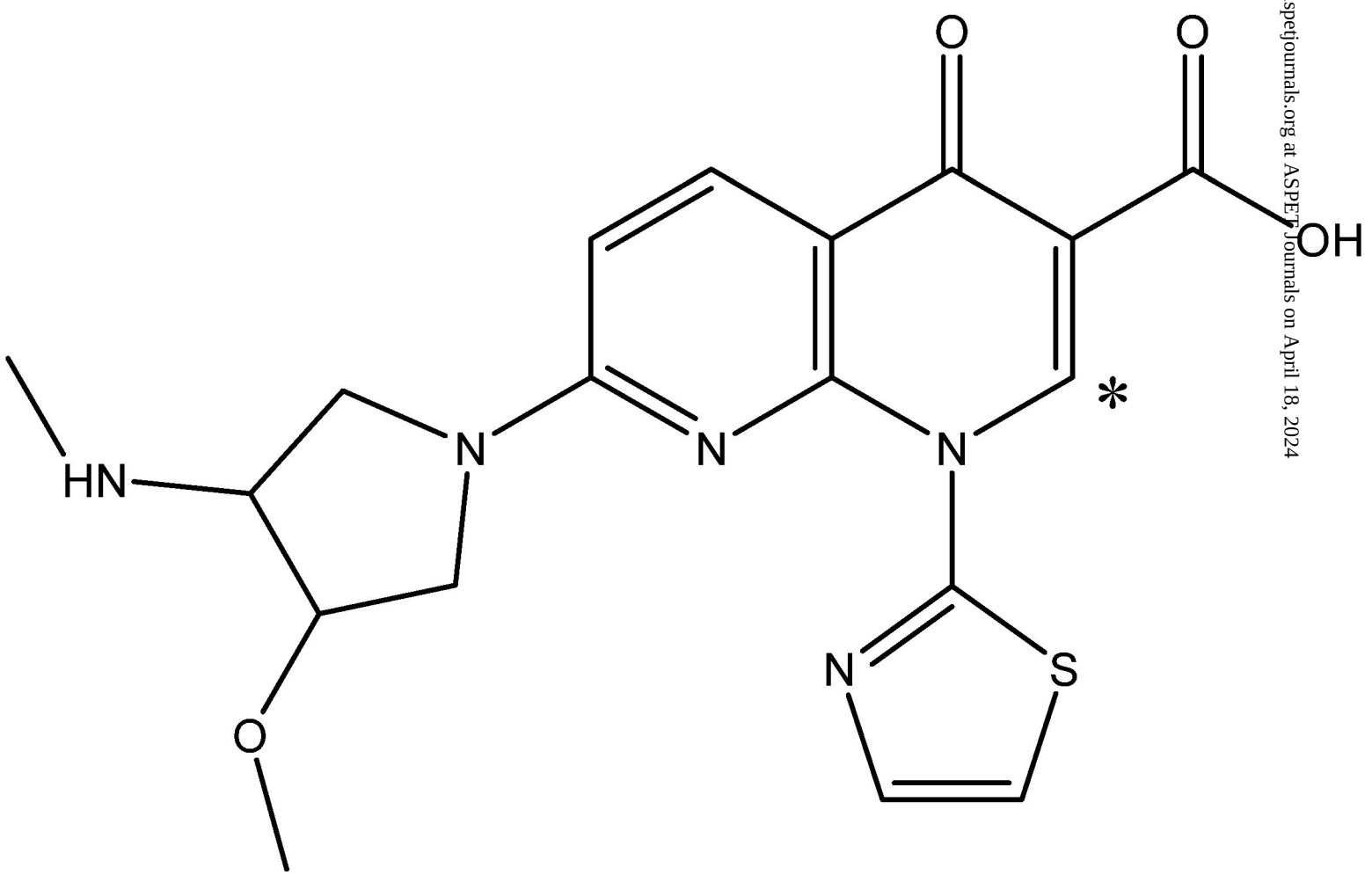

Figure 2

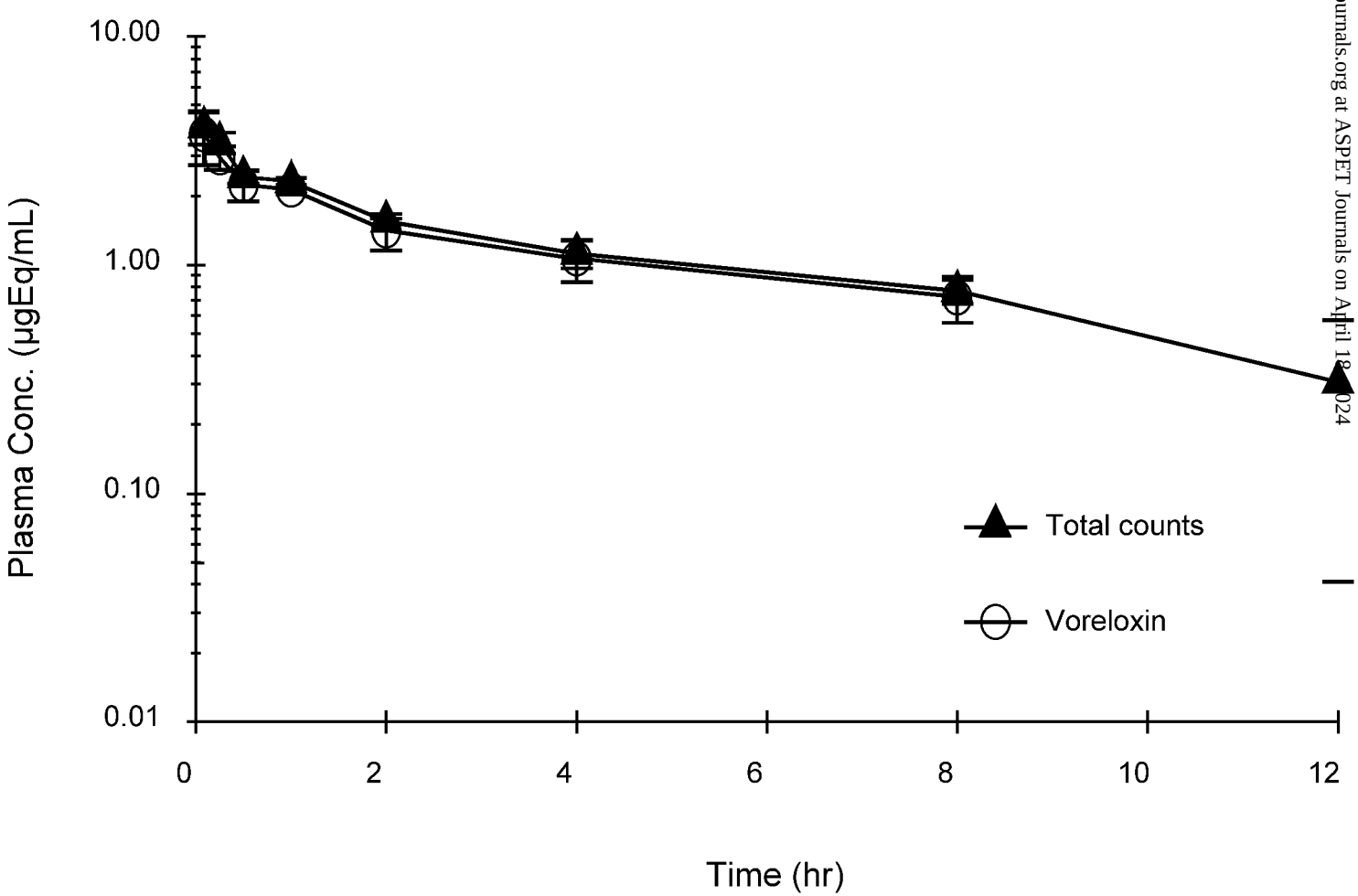

Figure 3

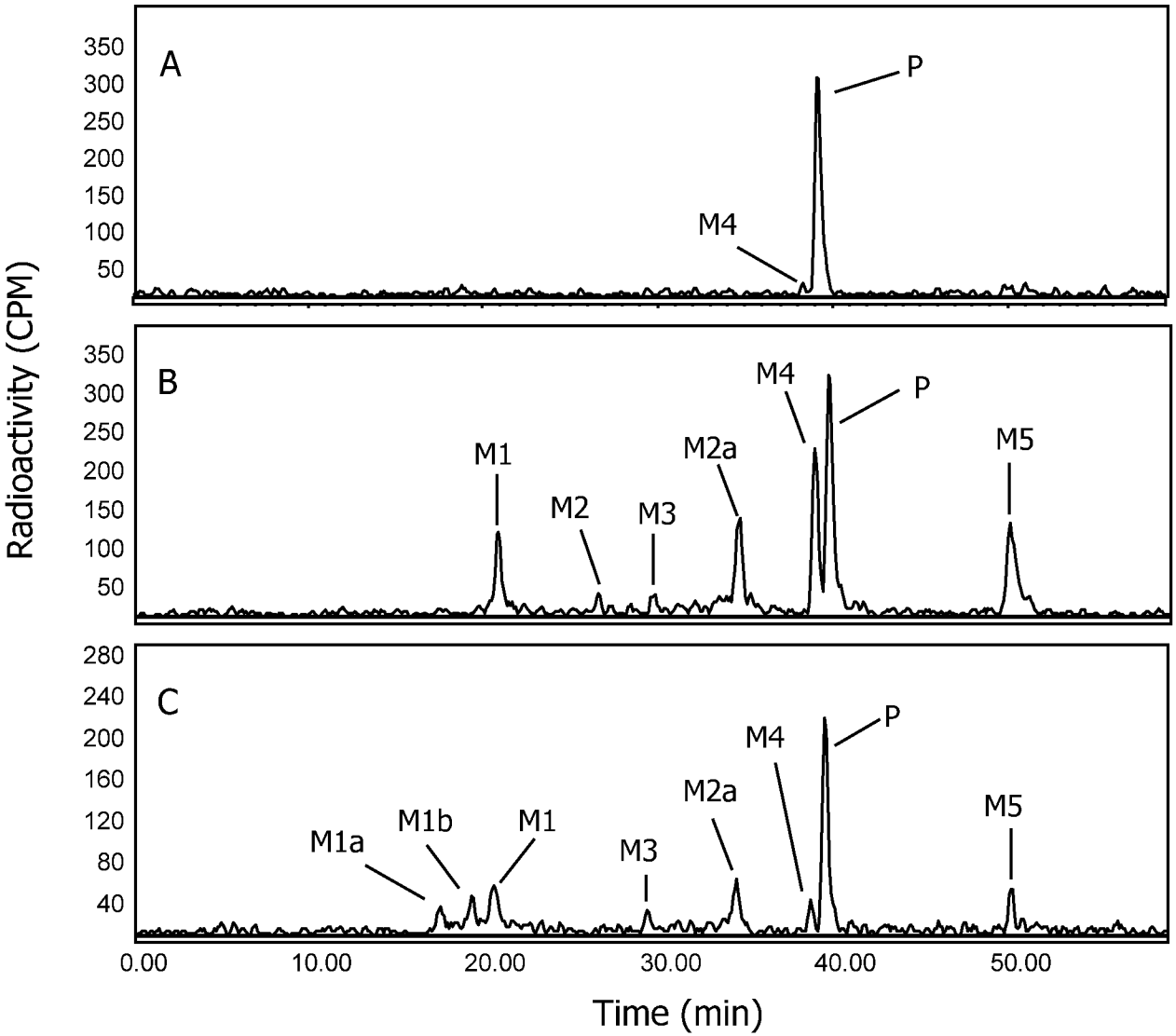

Figure 4

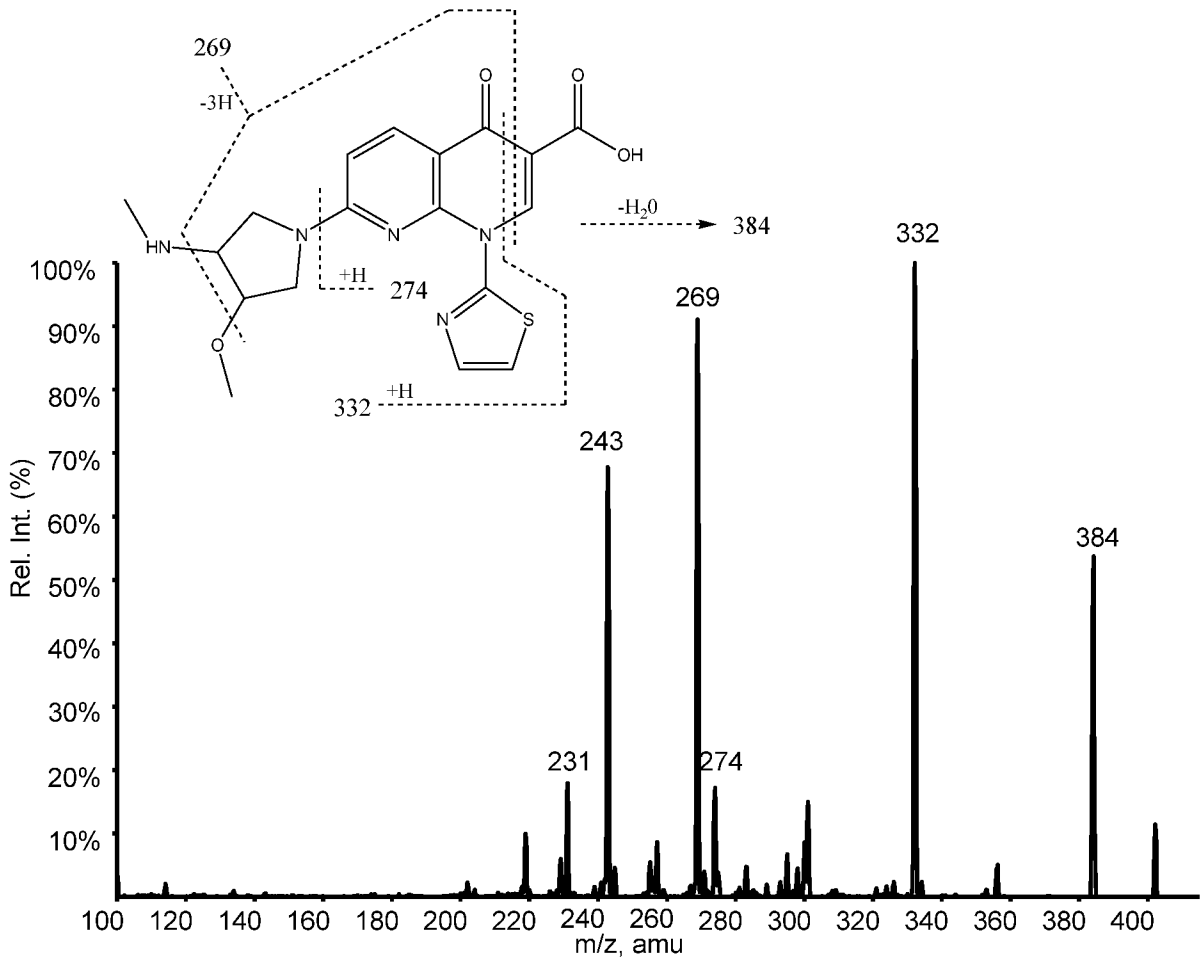

Figure 5